Compressible Turbulent Free Shear Layers

J. Craig Dutton
Department of Mechanical and Industrial Engineering
University of Illinois at Urbana-Champaign
Urbana, Illinois 61801 USA

1. ABSTRACT

Recent experimental work in the area of compressible turbulent free shear layers is reviewed. Results for the canonical two-stream, constant-pressure shear layer are given first. Emphasis is placed on growth rate, turbulence statistical quantities, large-scale turbulent structure, and growth rate enhancement. Compressible free shear layers present in high-speed separated flows are also considered. Here, results on mean flow, turbulence statistics, and large turbulent structures are discussed. Additional effects in these separated flows, such as the expansion that may occur at separation and the bulk compression, streamline curvature, and lateral streamline convergence that may occur at reattachment, are discussed. In order to develop a sound physical understanding of these compressible turbulent flows, particular attention is given to single-frame and multi-frame planar imaging studies.

2. INTRODUCTION AND MOTIVATION

Compressible free shear layers occur in a number of practical physical devices ranging from supersonic ejectors to gas dynamic and chemical lasers to the high-speed jets that are used for deposition of thermal spray coatings. However, the primary motivation for studying this flow in the last 10 years or so has been its importance for mixing the gaseous fuel and oxidant streams in supersonic combustors. Indeed, the major source of research funding for this problem in the U.S., especially during the mid- to late-1980s, was motivated by the desire to develop a scramjet-powered, single stage-to-orbit vehicle, such as the National AeroSpace Plane (NASP). However, since the demise of the NASP program, the volume of work addressing problems in this area has declined precipitously (at least in the U.S.). The timing of this AGARD/VKI Special Course on "Turbulence in Compressible Flows" therefore seems quite appropriate, as a review of progress made during the recent period of intense activity.

Compressible shear layers, although seemingly simple flows, are subject to quite complex fluid physics. The complications are partially due to the large Reynolds numbers, and consequent wide range of turbulent scales, that generally occur for gas flows under high-speed conditions. In addition, as will be shown abundantly below, compressibility itself has fundamental effects on turbulence that are not observed in low-speed flows. Nevertheless, considerable progress has been made in understanding compressible free shear layers in recent years. This progress has been facilitated both by the availability of vastly improved computational resources for numerical investigations and also by the development of non-intrusive laser-based diagnostic techniques for detailed experimental studies of this fundamental flow.

As might be expected, it would be impossible to thoroughly discuss all the recent accomplishments in the area of compressible free shear layers within the length constraints of this paper. Therefore, our primary objective is to review the physical understanding that has been developed through recent *experimental* studies of the *fluid dynamic* aspects of compressible shear layers. Reviews of numerical studies and topics such as scalar transport, mixing, and combustion are the subjects of other lectures in this Special Course. See also the recent review of Lele (1994) for a discussion of compressibility effects on turbulence with emphasis on analytical considerations and numerical results. The material presented here is certainly biased by our interests and experience at the University of Illinois in this general area. Therefore, we apologize in advance to any who might feel that their work has in any way been slighted or overlooked. Any errors of omission or commission are wholly the responsibility of the author.

3. CONSTANT-PRESSURE, TWO-STREAM, COMPRESSIBLE FREE SHEAR LAYERS

3.1 Dimensionless Parameters

Figure 1(a) is a schematic of a planar, matched-pressure, two-stream shear layer that is formed at the trailing edge of a splitter plate that separates the two streams. The subscript "1" will be used throughout to denote conditions of the higher speed stream, while subscript "2" refers to the lower speed stream. Thus, in the laboratory coordinates shown, the velocities of the freestreams are U_1 and U_2, their densities are ρ_1 and ρ_2, their speeds of sound are a_1 and a_2, their specific heat ratios are γ_1 and γ_2, and the static pressures at

Paper presented at the AGARD FDP Special Course on "Turbulence in Compressible Flows", held at the von Kármán Institute for Fluid Dynamics (VKI) in Rhode-Saint-Genèse, Belgium, 2-6 June 1997, and in Newport News, Virginia, USA, 20-24 October 1997, and published in R-819.

separation from the splitter plate are equal, $P_1 = P_2$. In the large body of work on *incompressible* mixing layers (*e.g.*, Brown and Roshko, 1974; Brown, 1978), it has been shown that the structure and behavior of the layer depend primarily on the freestream velocity ratio, $r = U_2/U_1$ [or, equivalently, the velocity parameter, $\lambda = (1-r)/(1+r)$], and the freestream density ratio, $s = \rho_2/\rho_1$.

To quantify the effects of *compressibility* on shear layers, Bogdanoff (1983) and Papamoschou and Roshko (1988) introduced the *convective Mach number*, M_c, which is the Mach number of the two freestreams relative to the large-scale structures in the mixing layer. To derive an expression for M_c, the layer is viewed in the reference frame that convects with the structures, Fig. 1(b). Assuming that the static pressures of the two streams are equal and that their (isentropically determined) total pressures are also equal at the stagnation point between structures in this frame, the following expression may be solved for the large-structure convection velocity, U_c

$$\left(1+\frac{\gamma_1-1}{2}\left(\frac{U_1-U_c}{a_1}\right)^2\right)^{\gamma_1/(\gamma_1-1)} = \left(1+\frac{\gamma_2-1}{2}\left(\frac{U_c-U_2}{a_2}\right)^2\right)^{\gamma_2/(\gamma_2-1)} \quad (1)$$

If $\gamma_1 = \gamma_2$, as is often the case in experimental studies, U_c is then given by

$$U_c = \frac{a_2U_1 + a_1U_2}{a_1 + a_2} \quad (2)$$

Using the definition of the convective Mach numbers of the two streams as their relative velocities with respect to the large structures divided by their speeds of sound gives

$$M_{c1} \equiv \frac{U_1 - U_c}{a_1} \quad \text{and} \quad M_{c2} \equiv \frac{U_c - U_2}{a_2} \quad (3)$$

If $\gamma_1 = \gamma_2$, the two convective Mach numbers are equal and can be written as

$$M_c = \frac{U_1 - U_2}{a_1 + a_2} \quad (4)$$

As mentioned above, this is the parameter that has been used overwhelmingly to quantify the effects of compressibility in mixing layers. It is often tacitly assumed that *all* the effects of compressibility are embodied in the magnitude of the convective Mach number. However, we must mention that there is evidence (*e.g.*, Sandham and Reynolds, 1989; Viegas and Rubesin, 1991) that the convective Mach number may be only a first-order measure of compressibility, *i.e.* that the effects of velocity ratio, density ratio, and/or other parameters may be different for compressible shear layers as compared to the incompressible case. In addition to r, s, and M_c, other "secondary" parameters that may influence the behavior of compressible mixing layers include: Reynolds number, state of the initial boundary layers, freestream turbulence, pressure gradients, and the compression and expansion waves that are virtually unavoidable in supersonic flow experiments.

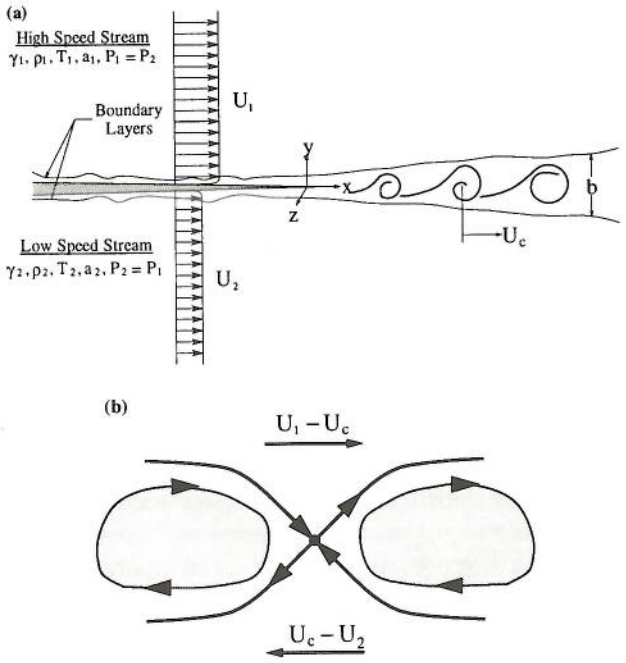

Fig. 1 Schematic of a two-stream mixing layer in (a) laboratory frame and (b) convective frame

3.2 Growth Rate

Perhaps the most well-known effect of compressibility on shear layers is the reduced growth rate that occurs as compared to that of incompressible mixing layers at the same velocity and density ratios. This is also an extremely important result in many applications, as mass *entrainment* from the freestreams into the layer, which results in its growth, is the first step in *mixing* the two streams (eventually at the molecular level so that chemical reactions can occur). Originally, the reduced growth rate effect was thought to be due to the density difference between the streams that occurs under compressible (versus incompressible) flow conditions. However, in their classic work on the subject, Brown and Roshko (1974) showed that the density effect was

small and that the growth rate reduction must be due to a separate and stronger compressibility effect.

In determining the growth rate of a shear layer, it is important that it be found only from the *fully-developed* or *self-similar* region. Goebel and Dutton (1991) studied the development of compressible mixing layers using the definition of Mehta and Westphal (1986) for fully-developed conditions: (1) linear growth rate with respect to downstream distance; (2) similarity of the mean velocity profiles when scaled by the local layer thickness; and (3) similarity of all turbulence quantity profiles when scaled by the local thickness, with peak turbulence quantities constant. Goebel and Dutton (1991) found that the mean velocity profiles required the least streamwise distance to become self-similar, followed by the streamwise turbulence intensity, transverse turbulence intensity, and Reynolds shear stress. By transforming Bradshaw's (1966) criterion for fully-developed single-stream shear layers to a criterion appropriate for two-stream layers, and by examining their experimental results for seven compressible mixing layer cases, Goebel and Dutton (1991) concluded that the following *approximate* local Reynolds number requirement must be met for full development

$$Re_b \equiv \frac{\overline{\rho}(\Delta U)b}{\overline{\mu}} \cong 1x10^5 \qquad (5)$$

where $\Delta U=U_1-U_2$ is the freestream velocity difference, b is the mixing layer thickness (defined below), and $\overline{\rho}$ and $\overline{\mu}$ are the average freestream density and viscosity, respectively. Note that Karasso and Mungal (1996) have recently found that the value of a "pairing parameter" better describes the development state of liquid plane shear layers, as compared to the local Reynolds number, although this result has not yet been extended to the compressible case.

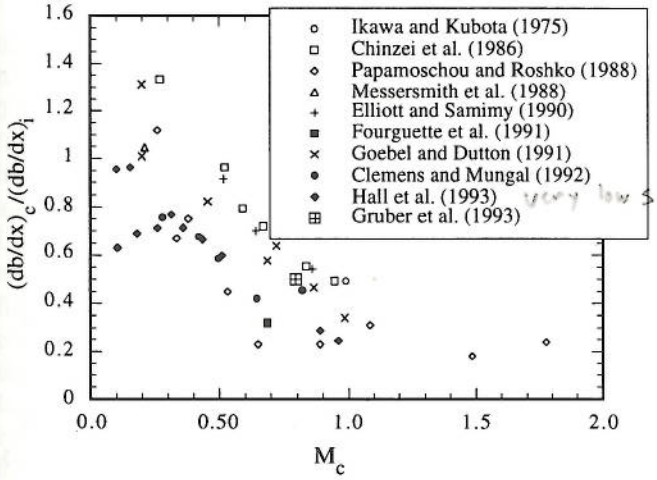

Fig. 2 Normalized growth rates of compressible mixing layers (from Gruber, 1992)

Figure 2 (from Gruber, 1992) shows the compressible mixing layer growth rate normalized by the incompressible growth rate at the same velocity and density ratios from some of the many studies that report this quantity. The incompressible growth rate for each case is determined from

$$\left(\frac{db}{dx}\right)_i = 0.165\lambda_s = 0.165\frac{(1-r)\left(1+s^{1/2}\right)}{2\left(1+rs^{1/2}\right)} \qquad (6)$$

where the constant has been suggested by Birch and Eggers (1972). It must be noted that many different definitions of the shear layer thickness are used in the literature. These include the 10%ΔU thickness, the vorticity thickness, the visual thickness, and the pitot thickness. We will usually use the 10%ΔU thickness, b, which is defined as the distance between transverse (y) locations where $U=U_1-0.1(\Delta U)$ and $U=U_2+0.1(\Delta U)$, see Fig. 1. All data presented in Fig. 2 have been transformed (assuming an error function mean velocity profile) to this common thickness definition.

As can be seen in Fig. 2, the normalized shear layer growth rate is indeed reduced as the compressibility of the layer, quantified by the convective Mach number, increases. In addition, these normalized data collapse moderately well when plotted against M_c. Possible reasons for the scatter in the data include differences in experimental techniques used to determine growth rate, lack of achievement of fully-developed conditions, differences in the thickness definition used and/or uncertainty in transforming to the "b" definition, and the possibility mentioned above that M_c provides only a first-order measure of compressibility. A few of the anomalous points in the figure deserve special mention. For example the high normalized growth rate reported at M_c=0.20 by Goebel and Dutton (1991) is due to "disturbed," high freestream turbulence conditions, which lead to an expected large growth rate. The low normalized growth rates reported by Hall *et al.* (1993) at low M_c are speculated by these authors to be due to poorly understood effects of very low density ratios coupled with a supersonic high-speed stream. In fact, the density ratios of these latter cases are lower than for any in the incompressible shear layer database, so that Eq. 6 may not accurately predict the growth rate used for normalization of these cases.

3.3 Turbulence Statistics

Because of the difficulties involved with making accurate, instantaneous velocity measurements in supersonic flows, few investigators have obtained

turbulence measurements in compressible shear layers. Elliott and Samimy (1990) studied three cases, Goebel and Dutton (1991) investigated seven cases, and Gruber *et al.* (1993) reported results for a single case. All of these measurements were obtained using laser Doppler velocimetry (LDV), where Elliott and Samimy (1990) and Goebel and Dutton (1991) presented two-component data and Gruber *et al.* (1993) obtained three-component results. Barre *et al.* (1994) have also presented one-component hot-wire anemometry (HWA) measurements for a compressible shear layer at M_c=0.62.

As discussed above in regard to the growth rate determination, it is critical that the turbulence measurements be reported from the fully-developed region, as the development of the layer immediately after separation from the splitter plate can depend strongly on the freestream and initial boundary layer conditions. This is especially true for the turbulence quantities, which have been found to develop more slowly than the mean velocity.

Figures 3-5 show averaged profiles from the fully-developed regions for five of the cases investigated by Goebel and Dutton (1991). The quantities plotted are the streamwise turbulence intensity, $\sigma_u/\Delta U$, the transverse turbulence intensity, $\sigma_v/\Delta U$, and the normalized kinematic Reynolds shear stress, $\langle u'v' \rangle/(\Delta U)^2$, respectively. (The symbol σ is used throughout to denote the rms fluctuation of the subscripted velocity component, and the angled brackets are used for ensemble-averaged quantities.) As expected, these turbulence quantities peak near the center of the shear layer and fall off to small values in the freestreams. In examining the effects of compressibility, increasing convective Mach number is seen to have a strong effect on reducing the magnitude of the transverse turbulence intensity and the Reynolds shear stress. We should note that the lowest compressibility case shown, M_c=0.20, may not have been fully developed, so that its profiles may be high in each case. With this caveat, the data shown in Fig. 3 indicate little effect of compressibility on streamwise turbulence intensity. Taken together, the trends for σ_u and σ_v, as measured by Goebel and Dutton (1991), suggest that the normal stress anisotropy, σ_u^2/σ_v^2, increases with increasing compressibility.

The effects of compressibility on the turbulence statistical quantities are more easily seen in Figs. 6-8, where the peak turbulence quantities from each of the four studies mentioned above have been plotted as a function of convective Mach number. In each case, the turbulence quantities have been normalized with respect to typical values measured for incompressible shear layers: $(\sigma_u/\Delta U)_i$=0.18, $(\sigma_v/\Delta U)_i$=0.13, and

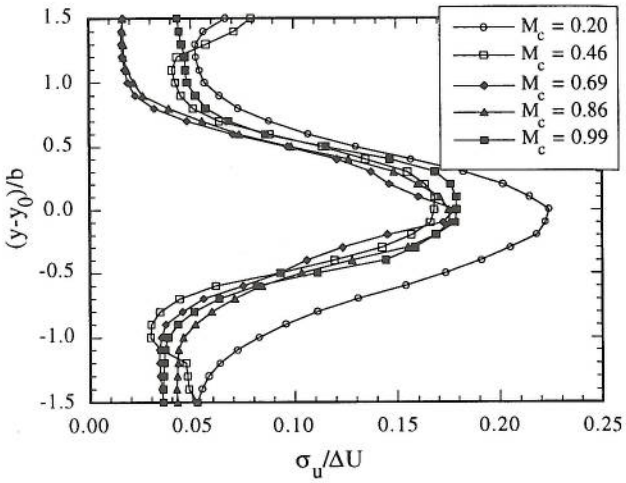

Fig. 3 Similarity profiles of streamwise turbulence intensity (from Goebel and Dutton, 1991)

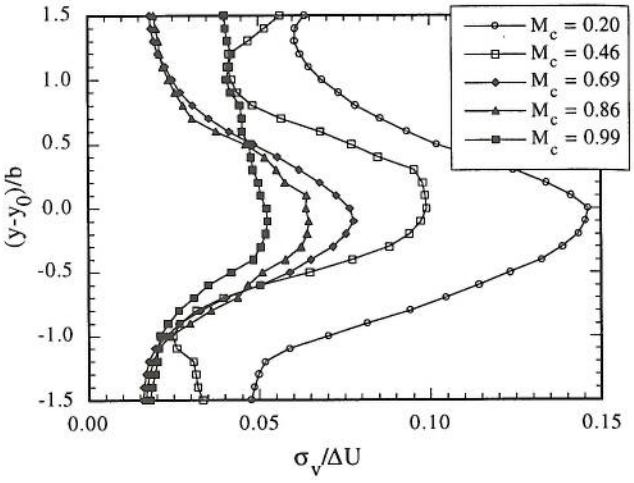

Fig. 4 Similarity profiles of transverse turbulence intensity (from Goebel and Dutton, 1991)

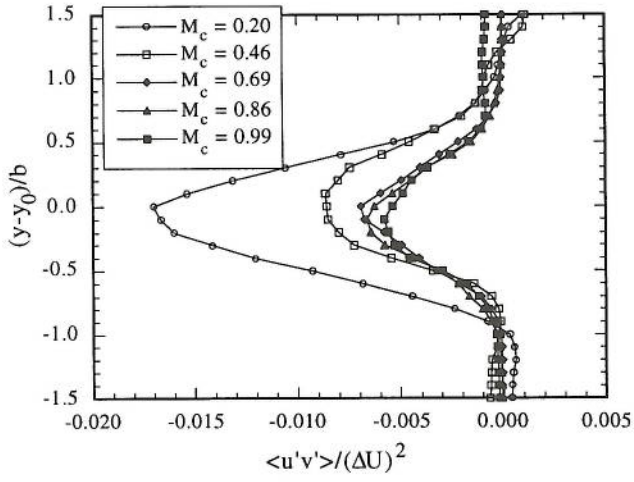

Fig. 5 Similarity profiles of normalized kinematic Reynolds stress (from Goebel and Dutton, 1991)

$(-\langle u'v'\rangle/(\Delta U)^2)_i=0.013$. The trends just mentioned from Goebel and Dutton (1991) are apparent: strongly reduced $\sigma_v/\Delta U$ and $-\langle u'v'\rangle/(\Delta U)^2$ and approximate constancy of $\sigma_u/\Delta U$ with increasing M_c. In addition, the data from all investigators for the peak transverse turbulence intensity and Reynolds shear stress collapse extremely well when plotted against convective Mach number. However, the data from Elliott and Samimy (1990) and Goebel and Dutton (1991) show some disagreement in the trends for the streamwise turbulence intensity. Instead of relatively constant values of $\sigma_u/\Delta U$ with increasing M_c, Elliott and Samimy (1990) found that this quantity also decreased, leading to a relatively constant normal stress anisotropy. In addition, these investigators found that the lateral (transverse direction) extent of the turbulence fluctuations within the shear layer is reduced as compressibility increases. Goebel and Dutton (1991), on the other hand, found no apparent reduction of the lateral extent of the turbulence fluctuations.

Gruber *et al.* (1993) reported three-component turbulence measurements for $M_c=0.80$. Their results for the streamwise and transverse turbulence intensities are in close agreement with Goebel and Dutton's (1991), which were obtained in the same facility. Gruber *et al.* (1993) found that the lateral extent of the turbulence profiles was reduced only on the high-speed side of the shear layer and that the peak spanwise turbulence intensity, $\sigma_w/\Delta U$, was about the same as for the incompressible case. Taken together with the reduced transverse turbulence intensity, the latter result implies that an effect of compressibility on the mixing layer is a tendency toward a more three-dimensional structure with enhanced spanwise, as compared to transverse, velocity fluctuations.

All three of the LDV studies consistently show that the shear stress correlation coefficient, $-\langle u'v'\rangle/(\sigma_u\sigma_v)$, is approximately constant, at a value between 0.4 and 0.5, both spatially within the shear layer and as a function of compressibility. This result provides an interesting turbulence model closure idea, which indeed has been utilized by Burr (1991). In addition, all of the LDV studies have shown that higher-order velocity moments, such as triple products, skewness, and flatness factors, are strongly reduced with increasing compressibility at the shear layer edges. This suggests that intermittency at the edges, due to excursions of large turbulent structures into the freestreams and, conversely, intrusions of inviscid freestream fluid into the shear layer, is also reduced.

We must emphasize that the discrepancies noted above for the streamwise turbulence intensity and lateral extent of the velocity fluctuations could be due to any

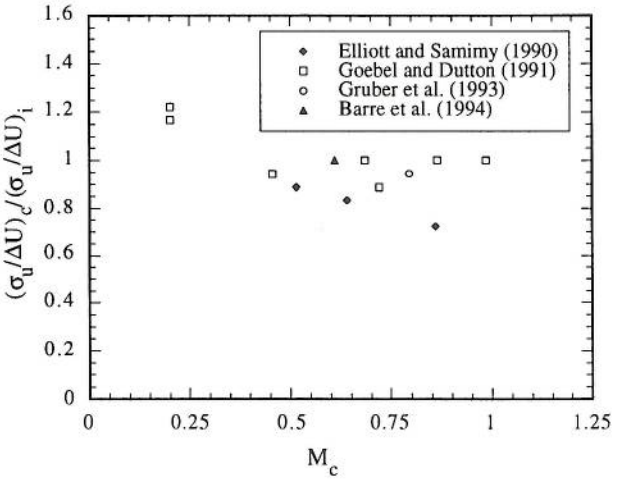

Fig. 6 Peak streamwise turbulence intensities from recent investigations (from Gruber *et al.*, 1993)

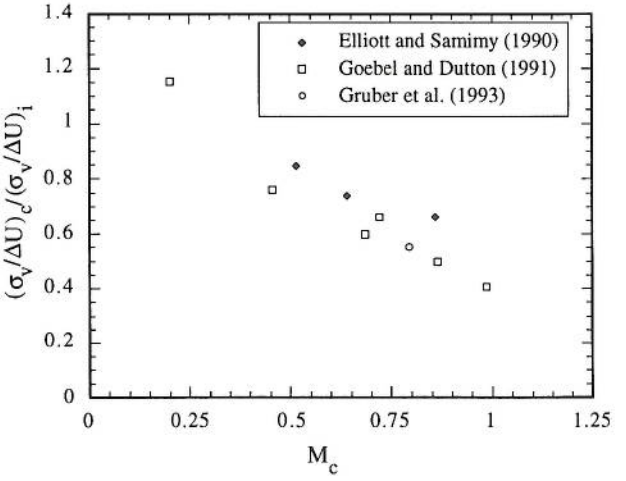

Fig. 7 Peak transverse turbulence intensities from recent investigations (from Gruber *et al.*, 1993)

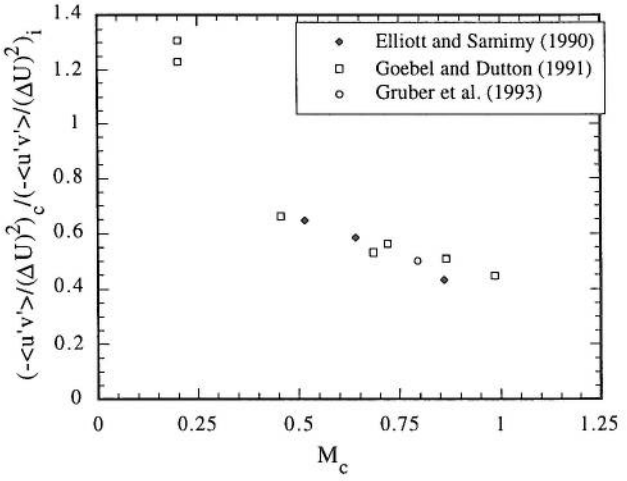

Fig. 8 Peak normalized primary Reynolds shear stresses from recent LDV investigations (from Gruber *et al.*, 1993)

of the secondary factors listed earlier or because the convective Mach number is not a complete descriptor of compressibility effects. Additional turbulence data, particularly at convective Mach numbers above about 0.8, are needed to clarify these issues. It is clear from the data presented that a primary effect of compressibility is a strong reduction of transverse velocity fluctuations and a trend toward a more three-dimensional turbulence structure, effects that will be reinforced by planar visualizations to be presented in the next section. In addition, inspection of Figs. 6-8 as a whole suggests better collapse of the normalized peak turbulence quantities when plotted against convective Mach number than for the normalized growth rate, Fig. 2, which is a surprising result.

3.4 Large-Scale Turbulent Structures

3.4.1 *Incompressible Shear Layer Structure*

As a prelude to discussing the large-scale organization of compressible shear layers, it is useful to first briefly review the structure of incompressible mixing layers. One of the landmark studies in this regard is that of Brown and Roshko (1974). In addition to investigating density ratio effects on shear layer growth rate, the shadowgraph visualizations of these authors clearly showed the dominant spanwise-oriented structures that exist in low-speed mixing layers, Fig. 9. These rolled-up structures develop from the fundamental Kelvin-Helmholtz instability of the flow. Since the time of Brown and Roshko's (1974) work, large-scale structures in turbulent shear flows have been the subject of a great deal of research. It has been found that these structures may pair, tear, and that they are stable, dominant features of low-speed shear layers even at high Reynolds numbers or in the presence of highly exothermic chemical reactions or other severe disturbances (Winant and Browand, 1974; Dimotakis and Brown, 1976; Wygnanski *et al.*, 1979). These structures have also been shown to be critically important in entrainment of the freestream fluids into the shear layer and to the cascade of turbulent scales that eventually results in mixing of the fluids at the molecular level (Dimotakis, 1986; Broadwell and Breidenthal, 1982; Broadwell and Mungal, 1988).

In addition to these spanwise structures, streamwise-oriented counter-rotating vortex pairs have been found to develop from the strain field induced by the spanwise rollers (Bernal and Roshko, 1986). These streamwise vortices, or ribs, are found in the braid region between the rollers with their ends wrapping around successive spanwise vortices; see Fig. 10 for an idealized schematic. The streamwise counter-rotating vortices induce fluid motion between them, either up or down, thus creating mushroom-shaped structures when viewed from the end (y-z plane, Fig. 1). The circulation of the streamwise ribs is found to be of the same order of magnitude as that of the spanwise rollers, suggesting that the interaction of the streamwise and spanwise vortices convolutes the layer interface and is responsible for significant entrainment and mixing between the two streams (Jimenez *et al.*, 1985).

3.4.2 *Schlieren and Shadowgraph Studies*

Against this backdrop for incompressible shear layers, it was only natural that early compressible mixing layer studies used schlieren and shadowgraph methods to investigate the existence of similar large-scale organization. This was done by several workers, *e.g.* Papamoschou and Roshko (1988), Elliott and Samimy (1990), Goebel and Dutton (1991), Clemens and Mungal (1992), and Hall *et al.* (1993). Figure 11 shows an example composite schlieren photograph of a compressible mixing layer at M_c=0.75 from the experiments of Messersmith (1992). As has been generally found in all other schlieren/shadowgraph studies, this figure shows, at best, only a slight hint of braided structure toward the downstream end, but certainly *not* the dominant, rounded, large-scale structures seen under incompressible conditions, Fig. 9. However, in drawing conclusions from these flow visualizations, we must remember that the schlieren and shadowgraph methods integrate effects along the line-of-sight, so that three-dimensionality (in the spanwise direction) of the turbulence structure will be smeared in the resulting photos.

3.4.3 *Probe-Based Structure Studies*

Time-series analyses of fluctuating pressure and hot-wire measurements have been used to investigate the structure and organization of compressible shear layers. Samimy *et al.* (1992) studied mixing layers at M_c=0.51 and 0.86 using fast-response pressure transducers. At the lower compressibility level, the measurements suggested that the large structures were similar to the incompressible case, with a predominantly two-dimensional spanwise orientation, although their spatial organization was poorer than for low-speed shear layers. At the higher compressibility, the structures were found to be highly three-dimensional in nature, with good spatial, but poor temporal organization. Figure 12, taken from this work, shows how much more strongly the streamwise coherence of the pressure fluctuations is reduced with increasing

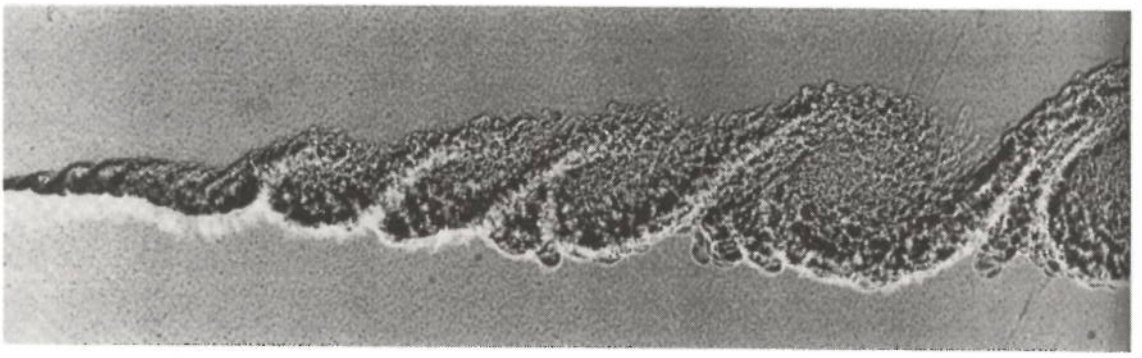

Fig. 9 Large-scale structure in an incompressible shear layer (from Brown and Roshko, 1974; as reproduced in Van Dyke, 1982)

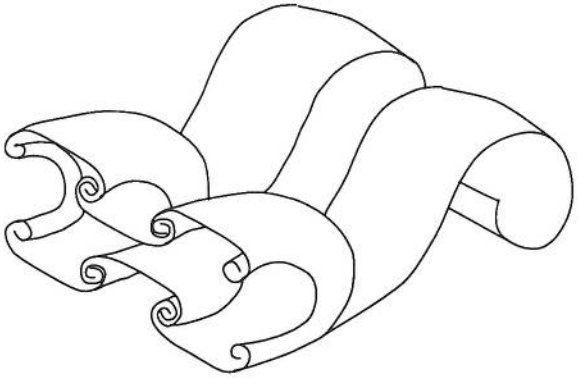

Fig. 10 Schematic of large-scale structure in an incompressible mixing layer: spanwise rollers and streamwise ribs (from Gruber, 1992)

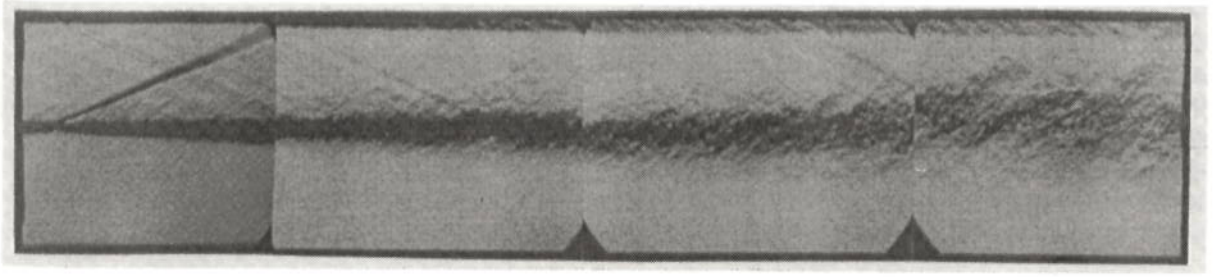

Fig. 11 Schlieren photograph of a compressible shear layer at M_c=0.75 (from Messersmith, 1992)

normalized probe separation distance, dx/δ_ω (where $\delta_\omega \approx b$), for M_c=0.86 than for M_c=0.51. This demonstrates a very strong effect of compressibility on the streamwise evolution of the structures. Spanwise correlation measurements were also suggestive of the existence of horseshoe-type vortices for the M_c=0.86 case.

Shau *et al.* (1993) and Petullo and Dolling (1993) used pressure fluctuation and dual normal hot-wire measurements, respectively, to investigate an M_c=0.28 shear layer formed between a Mach 5 and a Mach 3 stream. These measurements showed that the shear layer large structures were better organized than in the upstream boundary layer and that their organization increased with downstream distance, a finding that is in agreement with results of Samimy *et al.* (1992). Large-structure inclination angles of 35° to 55° to the streamwise direction were measured. All of the probe-based studies discussed here measured a broad range of structure angles for a given case, which is in agreement with the instantaneous planar images to be discussed below.

3.4.4 *Single-Frame Planar Imaging Results*

With the advent of laser diagnostic techniques, the line-of-sight integration limitation of the schlieren and shadowgraph methods could be removed, since thin laser sheets, generally of the order of a few hundred microns thickness, could be used to illuminate the flow. Techniques including Mie or Rayleigh scattering and planar laser-induced fluorescence (PLIF) were used in several studies of the turbulence structure of compressible shear layers (Clemens and Mungal, 1992, 1995; Elliott *et al.*, 1992; Bonnet *et al.*, 1993; Messersmith and Dutton, 1996; Poggie and Smits, 1996). Since pulsed lasers are used for these methods, the temporal resolution is also excellent, typically on the order of 10 ns, so that essentially "frozen" or "instantaneous" visualizations are obtained.

Example side-view (x-y plane, Fig. 1) Mie scattering images from the work of Clemens and Mungal (1995) are shown in Fig. 13 for a shear layer at M_c=0.28. These images utilize "product formation" seeding, in which ethanol vapor that is carried in the low-speed stream condenses into droplets only when molecularly mixed with cold fluid from the high-speed stream. This Mie scattering method therefore emphasizes large-structure cores where molecular mixing is expected to be most complete. The low compressibility case in Fig. 13 shows the existence of Brown-Roshko roller-like structures with connecting braids. The large structures and braids are most clearly seen in the downstream region of the images. Smaller-scale turbulence riding on the large-scale structures is also apparent, as might be expected for the large Reynolds number of this flow. Plan views (x-z plane, Fig. 1) of this same case are shown in Fig. 14. Here, the large structures are seen to be predominantly oriented in the spanwise direction and often span the entire field-of-view. However, skewing and bending with respect to the spanwise direction also occur frequently. Smaller streamwise-oriented structures connecting the spanwise rollers can also be observed.

Figures 15 and 16 show similar side and plan views of a compressible shear layer at M_c=0.62. The large structures visualized in the side view appear less well organized and are more jagged and irregularly spaced than those at lower compressibility. Clearly identifiable braids between large structures also appear to occur less frequently. The plan views show greatly

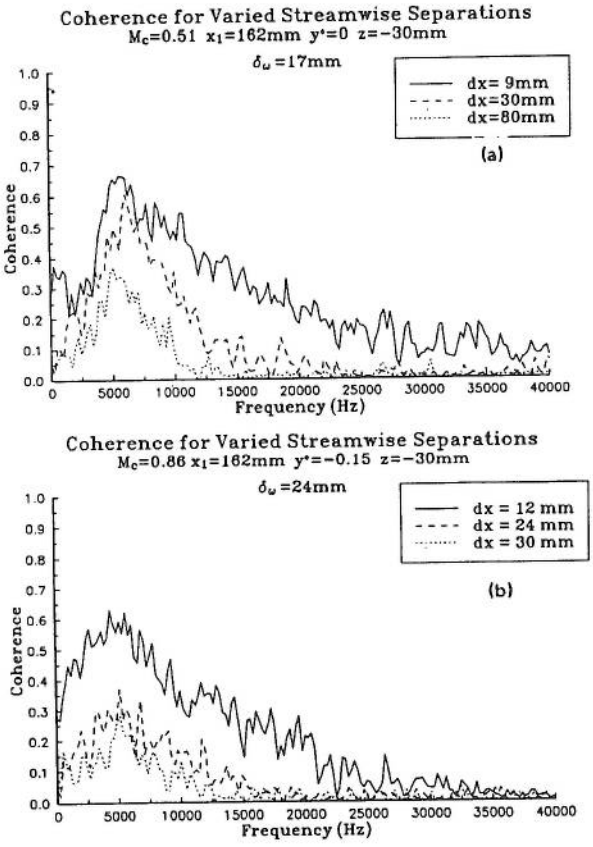

Fig. 12 Streamwise coherence for various probe separation distances for compressible shear layers at (a) M_c=0.51 and (b) M_c=0.86 (from Samimy *et al.*, 1992)